ACS OMEGA

Open Access



http://pubs.acs.org/journal/acsodf

Article

# Allyl Isothiocyanate Maintains DHA-Containing Glycerophospholipids and Ameliorates the Cognitive Function Decline in OVX Mice

Akika Nagata, Shiori Oishi, Nanako Kirishita, Keita Onoda, Takuma Kobayashi, Yuko Terada, Akira Minami, Nanami Senoo, Yasukiyo Yoshioka, Kunitoshi Uchida, Keisuke Ito, Shinji Miura, and Noriyuki Miyoshi*

Cite This: *ACS Omega* 2023, 8, 43118−43129

Read Online

ACCESS | Metrics & More | Article Recommendations | Supporting Information

**ABSTRACT:** Low-temperature-induced fatty acid desaturation is highly conserved in animals, plants, and bacteria. Allyl isothiocyanate (AITC) is an agonist of the transient receptor potential ankyrin 1 (TRPA1), which is activated by various chemophysiological stimuli, including low temperature. However, whether AITC induces fatty acid desaturation remains unknown. We showed here that AITC increased levels of glycerophospholipids (GP) esterified with unsaturated fatty acids, especially docosahexaenoic acid (DHA) in TRPA1-expressing HEK cells. Additionally, GP-DHA including phosphatidylcholine (18:0/22:6) and phosphatidylethanolamine (18:0/22:6) was increased in the brain and liver of AITC-administered mice. Moreover, intragastrical injection of AITC in ovariectomized (OVX) female C57BL/6J mice dose-dependently shortened the Δlatency time determined by the Morris water maze test, indicating AITC ameliorated the cognitive function decline in these mice. Thus, the oral administration of AITC maintains GP-DHA in the liver and brain, proving to be a potential strategy for preventing cognitive decline.

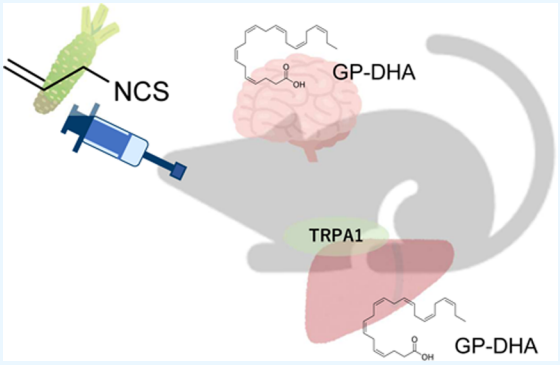


## INTRODUCTION

One of the most promising functional food factors, isothiocyanates (ITCs), are natural ingredients present in *Brassica* species, such as cabbage, broccoli, radish, mustard, and wasabi.[1,2] Sulforaphane, benzyl ITC, and phenethyl ITC are some of the well-studied ITCs. ITCs have several health benefits, including cancer chemoprevention,[3−6] anti-obesity,[7−10] anti-diabetic,[11−13] and anti-atherosclerosis[3,7] activities. ITCs covalently bind to the target proteins owing to their electrophilic nature and trigger multiple cell signaling pathways associated with various ITC-induced bioactivities.[1,14] Most importantly, Kelch-like ECH-associated protein 1 (Keap1), a critical target for ITCs to induce the antioxidant and xenobiotic-metabolizing enzymes, including NAD(P)H quinone oxidoreductase 1 (NQO1), glutathione S-transferase (GST), and glutamate-cysteine ligase catalytic subunit (GCLC), is regulated by the Keap1−nuclear factor-erythroid 2-related factor 2 (Nrf2) system.[15] Many other proteins have also been identified as targets for ITCs, such as tubulin for cell cycle arrest and apoptosis induction,[16,17] migration inhibitory factor for anti-inflammatory activities,[18−20] overexpressed MAPK/ERK kinase 1 in LNCaP cells for cell cycle growth inhibition,[21] recombinant topoisomerase II$\alpha$,[22] and other ubiquitously expressed proteins (such as the heat shock protein 90$\beta$, glyceraldehyde-3-phosphate dehydrogenase (GAPDH),[23] and albumin[24,25]). Transient receptor potential ankyrin 1 (TRPA1), an ion channel, is also a target for ITCs, especially allyl isothiocyanate (AITC).[26] TRPA1 is a chemosensor activated by various stimuli, including natural compounds (such as AITC), low temperature, calcium, hydrogen peroxide, gaseous molecules (such as $H_2S$ and NO), and oxidized lipids (such as 5,6-epoxyeicosatrienoic acid and 4-hydroxy-2-nonenal[27,28]). AITC is a strong agonist of TRPA1 *via* the covalent modifications of multiple cysteine residues.[29,30] TRPA1 is widely conserved in humans, mice, and several insects.[31,32] Although it is still controversial whether TRPA1 is a cold sensor, cold stimuli-induced lipid composition changes, especially fatty acid desaturation, have been observed in various bacteria,[33] plants,[34] and mammals.[35] However, whether AITC-induced TRPA1 activation causes changes in lipid composition has not yet been clarified.

**Received:** September 2, 2023
**Revised:** October 18, 2023
**Accepted:** October 19, 2023
**Published:** November 1, 2023

Many studies have reported the health benefits of *n*-3 polyunsaturated fatty acids (PUFAs), such as docosahexaenoic acid (DHA), eicosapentaenoic acid (EPA), and $\alpha$-linolenic acid (ALA), that are often consumed as diet supplements.[36,37] DHA plays an important role in the development and maintenance of brain function.[38,39] DHA constitutes 10−20% of the total lipids and is the most abundant *n*-3 PUFA (over 90%) in the brain.[40] The level of DHA in the brain decreases in an age-dependent manner, showing ∼22% reduction at 52−80 years compared with that at 29−35 years.[41] Age-dependent reduction in DHA is suggested to be strongly associated with cognitive function decline.[38,40] DHA is not synthesized *de novo* but can be converted from a precursor ALA *via* sequential metabolism comprising desaturation and elongation in the endoplasmic reticulum and $\beta$-oxidation in the peroxisomes. However, the capacity of the human brain for DHA biosynthesis from ALA is very low, estimated to be less than 1%. Brain DHA is mainly synthesized in the liver and transported through the bloodstream.[42] DHA supplementation increases blood DHA levels but does not show clear beneficial effects on mild cognitive impairment, dementia, and Alzheimer's disease.[43−45] The administration of 6-(methylsulfinyl)hexyl ITC (6-MSITC) was found to improve impaired cognition in the Alzheimer's disease model $App^{NLGF}$ mice by suppressing oxidative stress and neuroinflammation *via* the Nrf2-Keap1 pathway.[46] However, the association of brain cognitive functions with ITC-induced lipid composition changes has not yet been determined. Therefore, it is not clear whether AITC induces PUFAs and whether AITC-induced PUFAs contribute to brain functions.

In this study, we evaluated whether AITC-TRPA1 signaling induced changes in lipid composition *in vitro* and *in vivo*. Lipidomics analysis based on liquid chromatography−mass spectrometry (LC-MS) was performed to evaluate the lipid composition changes, especially focusing on the level of unsaturation (the number of unsaturated double bonds) of fatty acids in phospholipids. We found that AITC increased the levels of DHA-acylated phospholipids *via* the TRPA1 signaling pathway in TRPA1-expressing HEK cells. Moreover, the elevated levels of DHA-acylated phospholipids in the brain and liver of AITC-administered mice may be involved in the improvement of ovariectomy (OVX)-induced cognitive decline in the brain. These results indicate that DHA uptake from dietary supplements and an increase in DHA-containing lipids may be potential preventive strategies for mild cognitive impairment in aging.

## MATERIALS AND METHODS

**Cell Culture.** T-REx™-293 cells (Thermo Fisher Scientific, Waltham, MA) derived from HEK293 cells were stably transfected with a tetracycline-regulating TRPA1 expression vector to prepare human TRPA1-expressing cells (HEK_hTRPA1 cells), as previously described.[47−49] HEK_hTRPA1 cells were maintained in Dulbecco's modified Eagle's medium (Nissui Pharmaceutical Co. Ltd., Tokyo, Japan) supplemented with 10% fetal bovine serum, 100 U/mL penicillin, 100 $\mu$g/mL streptomycin, 500 $\mu$g/mL zeocin, and 10 $\mu$g/mL blasticidin. HEK(−) cells were cultured at 37 °C in a 5% $CO_2$ humidified incubator and passaged twice a week. TRPA1 expression was induced by the addition of 1 $\mu$g/mL tetracycline for 24 h. After loading Fluo-4 AM (Thermo Fisher Scientific), TRPA1 activity was confirmed using a FlexStation II microplate reader system (Molecular Devices, Sunnyvale, CA).[47−49] Cytotoxicity of AITC was determined using the AlamarBlue assay, as described previously.[50,51]

**Lipidomics Analysis.** Lipidomics analyses were performed as described previously.[52,53] For lipid extraction from HEK_hTRPA1 cells, the cell pellet harvested from a 3.5 mm dish was sonicated in 150 $\mu$L of MeOH and 500 $\mu$L of methyl *tert*-butyl ether (MTBE), containing 50 $\mu$g/mL 1,2-diheptadecanoyl-*sn*-glycero-3-phosphocholine (DHDPC) and 0.2 mg/mL dibutylhydroxytoluene (BHT). Samples were incubated in a shaker at 1500 rpm for 1 h at room temperature, combined and vortexed with 125 $\mu$L ultrapure water (MQ), and left to stand for 10 min. After centrifugation at 100*g* for 10 min at 4 °C, the organic phases were separated and washed with 150 $\mu$L of MeOH, 500 $\mu$L of MTBE, and 125 $\mu$L of MQ. The organic phases were combined with the former and then dried using a centrifuge evaporator. The residues were dissolved in 100 $\mu$L of MeCN/IPA/MQ (65:30:5, v/v/v). For the lipid extraction from mouse tissues, 10 mg (wet weight) of brain or liver in 100 $\mu$L of MQ was microdestructed (2500 rpm, 4 °C, 20 s) by MicroSmash MS-100R (TOMY, Japan) with a 5.0 $\varphi$ zirconia ($ZrO_2$) bead. Aliquots (50 $\mu$L) of the homogenate were collected in new tubes and mixed with 100 $\mu$L of MeOH and 500 $\mu$L of MTBE, containing 50 $\mu$g/mL DHDPC and 0.2 mg/mL BHT. Samples were incubated in a shaker at 1500 rpm for 1 h at room temperature, combined, and vortexed with 75 $\mu$L of MQ, and then left to stand for 10 min. After centrifugation at 100*g* for 10 min at 4 °C, the organic phases were separated and washed with 30 $\mu$L of MeOH, 100 $\mu$L of MTBE, and 25 $\mu$L of MQ. The organic phases were combined with the former and then dried using a centrifuge evaporator. The residues were dissolved in 100 $\mu$L of MeCN/IPA/MQ (65:30:5, v/v/v).

Extracted lipids were analyzed using LC-MS consisting of AQUITY UPLC (Waters, Milford, MA) coupled with micrOTOFQII (Bruker Daltonics, Bremen, Germany). Ultra-performance liquid chromatography (UPLC) separation[54,55] was performed with a TSKgel ODS-120H column (1.9 $\mu$m, 50 mm × 2.0 mm i.d., TOSOH) at 40 °C, using solvent A (60:40 MQ/MeCN in 5 mM ammonium formate and 0.1% formic acid) and solvent B (90:10 IPA/MeCN in 5 mM ammonium formate and 0.1% formic acid). The samples were eluted from the column using a linear gradient of 10% solvent B at 0 min, 50% solvent B at 1 min, and 70% solvent B at 20 min. The flow rate of the mobile phase was 0.4 mL/min. Quadrupole time-of-flight mass spectrometry (Q-TOF-MS) was operated in negative-ion mode using an electrospray ionization source. The detector conditions were as follows: capillary voltage, 3900 V; nebulizer, 2.0 bar, drying gas flow, 10 L/min; drying gas temperature, 200 °C; mass range, 50−1500 $m/z$. All analyses were performed by using a sodium formate solution (5 mM NaOH and 0.1% formic acid in 50% MeOH) to accurately calibrate the mass. MS peak data from UPLC-TOF-MS analyses were subjected to Compass Data Analysis (Bruker) and Signpost (Reifycs, Tokyo, Japan) for peak detection and integration, and Mass Profiler Professional software (Agilent Technologies) was used for principal component analysis. To identify the lipid species, MS/MS spectra obtained with a CID of 30 eV were searched against the LIPID MAPS database (https://www.lipidmaps.org/).

**Morris Water Maze Test.** All animal experimental protocols were approved by the Animal Ethics Committee of the University of Shizuoka (approval number 205289) and performed according to the ARRIVE guidelines. Eight-week-


https://doi.org/10.1021/acsomega.3c06622
ACS Omega 2023, 8, 43118−43129

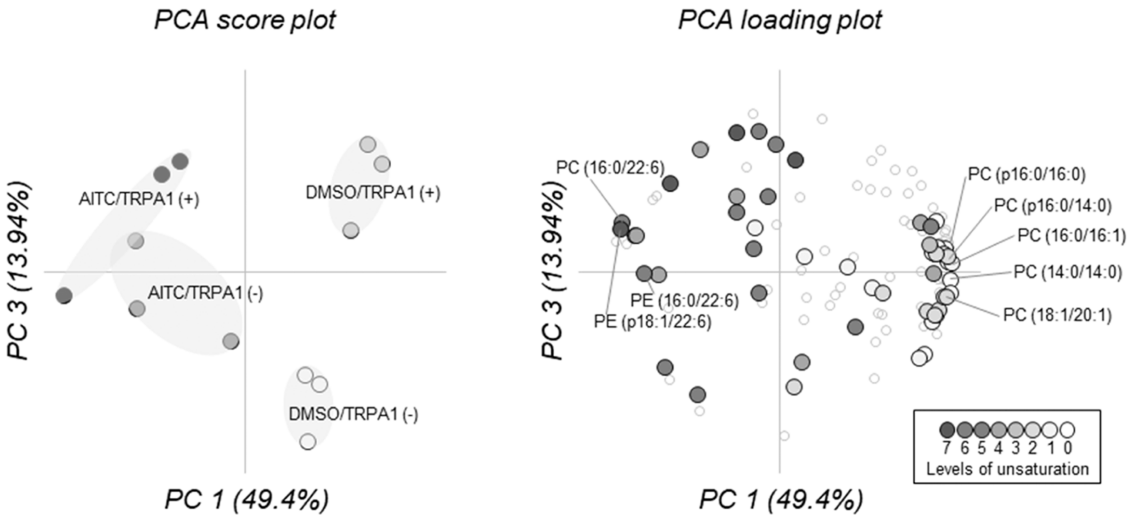


**Figure 1.** AITC induced *n*-3 polyunsaturated fatty acid (PUFA)-acylated phospholipids *via* the TRPA1 pathway in HEK_hTRPA1 cells. HEK_hTRPA1 cells were treated with or without tetracycline for 24 h to induce TRPA1 expression and exposed to 10 $\mu$M AITC or dimethyl sulfoxide (DMSO) (vehicle). The extracted lipid fractions were subjected to lipidomics analysis. On the principal component analysis (PCA) score plot, four experimental groups, including ATIC/TRPA1 (+), DMSO/TRPA1 (+), ATIC/TRPA1 (−), and DMSO/TRPA1 (−), were individually surrounded by a gray ellipse. On the PCA loading plot, edged circles indicate the identified phospholipids. Levels of unsaturation (the number of unsaturated double bonds) are shown by a black and white gradation. Unidentified lipid molecules are shown by small light gray circles.

old female C57BL/6J mice were purchased from Japan SLC (Hamamatsu, Japan). All animals were fed a standard chow diet (MF; Oriental Yeast, Co., Ltd., Tokyo, Japan), housed in plastic cages, and had free access to drinking water under controlled conditions of humidity (55 ± 5%), light (12/12 h light/dark cycle), and temperature (23 ± 1 °C). Fatty acid composition in MF diet used in this study was shown in Supporting Table S1. After a 1-week adaptation period, mice were subjected to either ovariectomy (OVX) or a sham operation (on day 7). After 10 days of recovery from the surgical operation, AITC (0, 1, or 10 mg/kg body weight) in a suspended solution (dimethyl sulfoxide (DMSO):Tween 80:saline = 5:10:85) was intragastrically injected every day until the end of the experiment (on days 18−35). The Morris water maze test[56] was started on day 30 using mice (total $n$ = 32) grouped in Sham ($n$ = 6), Sham + AITC (10) ($n$ = 6), OVX ($n$ = 7), OVX + AITC (1) ($n$ = 6), and OVX + AITC ($n$ = 7), which were prepared by the above method. A transparent platform was installed under the water surface in a pool (120 cm diameter) filled with water (22 ± 2 °C). Each mouse was placed in the pool, and the time taken to reach the platform was measured (up to a maximum of 40 s). Four trials were performed on 1 day at 1 min intervals, and this was repeated for 5 d. The locations of the mice in the pool were randomly changed after each trial. Memory of the platform location was assessed by quantifying the mean latency to reach the platform on day 5. In the initial trial on day 1, the pool was virtually divided into four divisions (north, south, east, and west), and the number of times the mice crossed each division was measured to evaluate their motility. If mice got to the platform by chance, the number of crossings was corrected to the number of crossings per 40 s. The behavior of the mice during the experiment was recorded by using a video camera (GoPro Inc., San Mateo, CA). The latency time to reach the platform and motility in the Morris water maze test were measured by analyzing the video data using a video tracking system (ANY-maze version 5.3; Muromachi Kikai, Tokyo, Japan).

**Reverse Transcription-Quantitative Polymerase Chain Reaction (RT-qPCR).** Cells cultured in a 35 mm dish were washed twice with ice-cold phosphate-buffered saline (PBS) (pH 7.4), 1 mL of TRIzol reagent (Invitrogen), and collected using cell scraper. Total RNA was extracted according to the manufacturer's protocol and converted into cDNA using the PrimeScript RT Master Mix (TaKaRa Bio, Japan). To quantitatively estimate the expression level of each gene, qPCR was performed using gene-specific primers, cDNA, and SYBR Premix (TaKaRa Bio). The sequences of the PCR primer pairs used were as follows: m*GAPDH*: 5′-AAA ATG GTG AAG GTC GGT GTG-3′ and 5′-AAT GAA GGG GTC GTT GAT GG-3′; mouse ELOVL fatty acid elongase 2 (m*Elovl2*): 5′-ACC GGA AAA AGC CAG TGA AG-3′ and 5′-TTG TCC GTC ATG CCA TTA GC-3′; m*Elovl5*: 5′-TTT TTC TGC CAG GGA ACA CG-3′ and 5′-TGG TGG TTG TTC TTG CGA AG-3′; mouse fatty acid desaturase 1 (m*Fads1*): 5′-ATG CAT TTC CAG CAC CAT GC-3′and 5′-TGT GCT GAT GGT TGT ATG GC-3′; m*Fads2*: 5′-TTT CCA ACA CCA TGC CAA GC-3′ and 5′-TCG CCA AGG ACA AAC ACA TG-3; mouse 1-acylglycerol-3-phosphate *O*-acyltransferase 3 (m*AGPAT3*/m*LPAAT3*): 5′-TCA TTG GCT TCG TCT TCG TG-3′and 5′-ATA CGG CGG TAT AGG TGC TTG-3′; mouse acyl-CoA synthetase long-chain family member 6 (m*ACSL6*): 5′-TCG GGC TTT CTG AAA GTG AC-3′ and 5′-ACC ATG CGC TCA AAC ATG TG-3′.

**Statistical Analysis.** All data are presented as the mean ± standard error of the mean (SEM). All statistical analyses were performed using EZR (Saitama Medical Center, Jichi Medical University), a graphical user interface for R (The R Foundation for Statistical Computing). Statistical analyses of data were performed using the Student's $t$-test, one-way analysis of variance (ANOVA) followed by Tukey honest significant difference post hoc test, or two-way ANOVA with multiple testing correction using the Bonferroni family-wise error rate. Differences were considered to be statistically significant at $P < 0.05$.


https://doi.org/10.1021/acsomega.3c06622
ACS Omega 2023, 8, 43118−43129

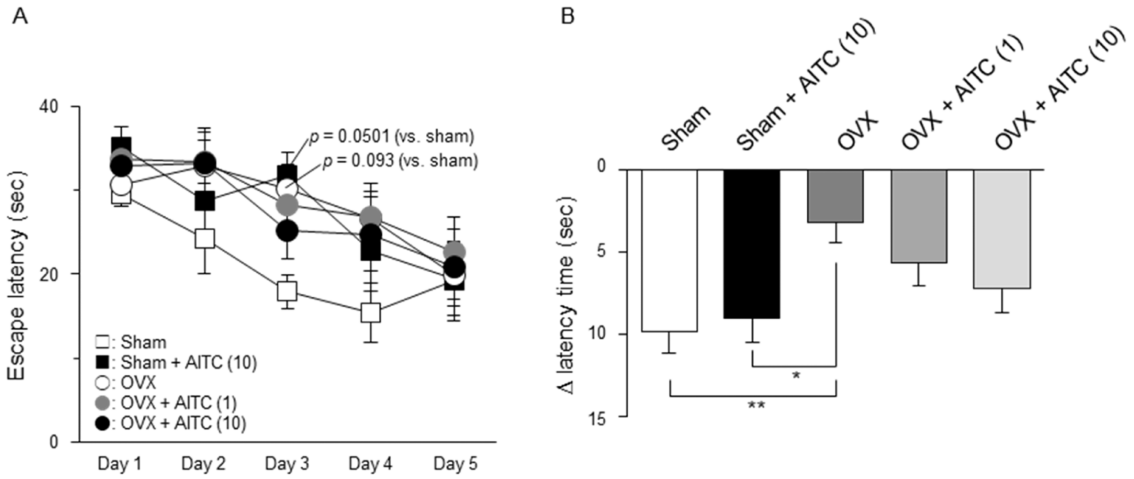


**Figure 2.** AITC ameliorated ovariectomy (OVX)-induced cognitive function impairment. Female C57BL/6J mice that received sham or OVX operation were intragastrically injected with AITC for 18 d. Morris water maze tests were performed to evaluate the spatial cognitive function on the last 5 d of the experiment. (A) The escape latency time was measured for 5 d. Values are represented as the mean ± SEM ($n$ = 6 or 7 mice/groups × 4 trial/day). Statistical significance was determined by two-way repeated analysis of variance (ANOVA) and one-way ANOVA followed by Tukey honest significant difference (HSD) post hoc test. (B) The delta time (Δlatency time) was adjusted by averaging the difference between the score of day 0 and the respective scores of days 2−5. Values are represented as the mean ± SEM ($n$ = 6 or 7 mice/groups × 4 trial/day). Statistical significance was determined by one-way ANOVA followed by Tukey HSD post hoc test. *$P$ < 0.05 and **$P$ < 0.01.

## RESULTS

**AITC Increased the Levels of PUFAs in TRPA1-Overexpressing HEK Cells.** To investigate the agonistic activities of AITC, we prepared HEK cells with TRPA1 expression regulated by the tetracycline system, hTRPA1(+) and HEK_hTRPA1(−), were prepared. We confirmed that up to 10 $\mu$M AITC treatment induced TRPA1 activation without cytotoxicity.[48] Lipid fractions prepared from hTRPA1(+) and HEK_hTRPA1(−) cells treated with 10 $\mu$M AITC or DMSO (vehicle) were subjected to lipidomic analysis, which detected 119 phospholipid molecules, 52 of which were identified (Supporting Table S2). As shown in Figure 1, four experimental groups including AITC- or DMSO (vehicle) treated HEK_hTRPA1(+) and HEK_hTRPA1(−) cells, respectively, were distributed on score plot. The distribution along PC1 was dependent on AITC treatment, and PC3 separation was dependent on TRPA1 expression. The AITC/TRPA1 (−) group was located relatively close to AITC/TRPA1 (+), possibly due to the leakage of TRPA1 expression in the tetracycline system. The loading plot demonstrated that the level of unsaturation in the fatty acid residues of phospholipids was apparent along PC1. The location of DHA (22:6)-containing phospholipids, such as PC (16:0/22:6), PE (16:0/22:6), and PE (p-18:1/22:6), was strongly associated with the distribution of the AITC/TRPA1 (+) group (Figure 1). On the other hand, many phospholipids with lower levels of unsaturated fatty acid residues, such as PC (14:0/14:0) and PC (16:0/16:1), were located in the opposite area of AITC/TRPA1 (+). Additionally, 10 $\mu$M AITC hardly induced genes regulated by Nrf2, including NQO1, GCLC, and GSTP1 in AITC/TRPA1 (+) cells (Supporting Figure S1). These results suggest that AITC induces phospholipids containing unsaturated fatty acid residues in HEK_hTRPA1-(+) cells, depending on the TRPA1 pathway rather than the Keap1/Nrf2 pathway.

**AITC Ameliorated the Decline in Cognitive Function in OVX Mice.** Although the extent to which central nervous system functions are affected in postmenopausal women is not clear,[57] ovariectomy (OVX) have a negative effect on cognitive function, including attention, learning, and memory.[58−60] Additionally it was also observed that the level of hepatic DHA was slightly decreased in OVX rats.[61] Since DHA is important for maintaining brain function,[62] whether AITC-induced lipid composition changes influenced cognitive functions was investigated. AITC (1 or 10 mg/kg body weight) or vehicle was intragastrically injected every day into ovariectomized or sham mice until the end of the experimental period. On the last 5 days, Morris water maze tests were performed to evaluate spatial cognitive function. Body weight on days 25 and 29 in OVX and OVX + AITC 10 groups were significantly higher than sham mice, indicating that loss of ovarian hormones influences body weight (Supporting Figure S2A). In all experimental groups, escape latency times gradually decreased as the daily tests were repeated (Figure 2A). In particular, the sham group seemed to have shown an efficient learning effect, although statistical significance ($P$ < 0.05) was not observed in the escape latency time among the experimental groups (Figure 2A). However, as shown in Figure 2B, the sham and sham + AITC (10) groups demonstrated significantly superior scores in delta (Δ) latency time compared to the OVX group. Moreover, AITC improved the Δlatency in ovariectomized mice in a dose-dependent manner (Figure 2B). There was no difference in tissue weight of hippocampus and cerebral cortex collected on day 35 (Supporting Figure S2B). These results suggest that the oral administration of AITC affects cognitive function in the mouse brain.

**Compositional Changes in Lipids in the Brain and Liver of AITC-Administered Mice.** To explore the involvement of AITC in improving cognitive function decline in OVX mice with changes in lipid composition, brain (hippocampus and cerebral cortex) and liver samples were prepared after Morris water maze tests. Lipid fractions were extracted, injected into LC-MS, and analyzed by principal component analysis (PCA). In the score plot in Figure 3A, ovariectomized mice grouped as OVX, OVX + AITC (1), and OVX + AITC (10) were distributed in a different area than


https://doi.org/10.1021/acsomega.3c06622
ACS Omega 2023, 8, 43118−43129

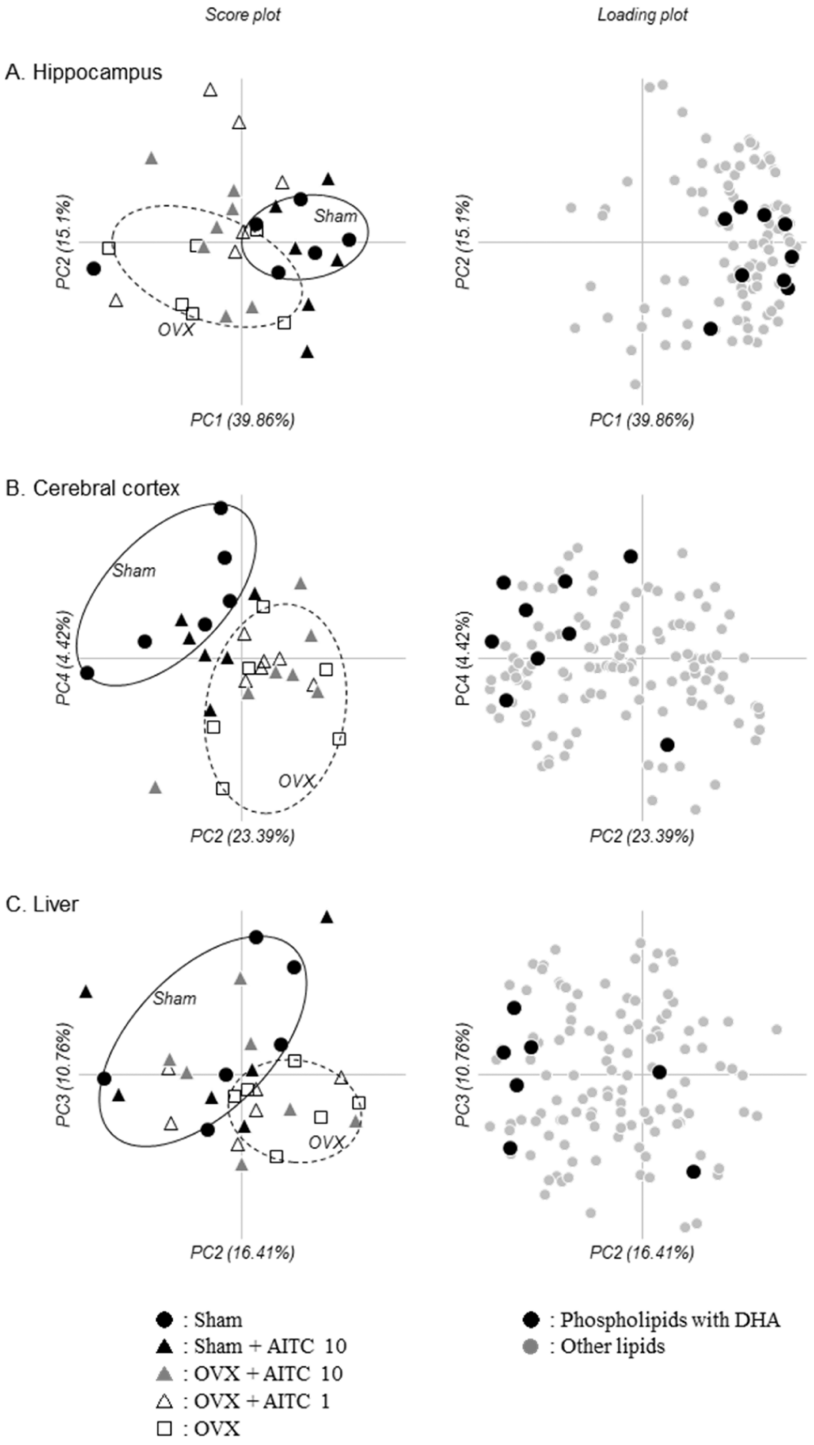


**Figure 3.** AITC administration induced the phospholipids containing docosahexaenoic acid (DHA). C57BL/6J mice were subjected to OVX or sham operation. After 10 d of recovery, intragastric injections of AITC (0, 1, or 10 mg/kg body weight) were given daily for 18 d. Lipid fractions prepared from the hippocampus (A), cerebral cortex (B), and liver (C) were analyzed by liquid chromatography−mass spectrometry (LC-MS), and PCA was performed. Mice grouped in sham (●), sham + AITC 10 mg/kg bw (▲), OVX (□), OVX + AITC 1 mg/kg bw (△), and OVX + AITC 10 mg/kg bw (▲) were shown in PCA score plots. Sham groups are circled by solid lines and OVX groups are circled by dashed lines. On the PCA loading plot, phospholipids containing DHA are shown by closed black circles and others by small light gray circles.

sham-operated mice. In particular, the OVX group was distributed along the PC1 axis from the sham group. The OVX + AITC (1) and OVX + AITC (10) groups showed a merging distribution between the OVX and the sham groups. The loading plot showed that nine phospholipids containing DHA contributed to the distribution of the sham and sham AITC (10) groups. PE (18:1/22:6), PC (16:0/22:6), PE (16:0/22:6), and PE (18:0/22:6) were strong contributors to PC1 (Table 1). In the cerebral cortex and liver, the OVX and sham groups were clearly separated along the principal component axes (Figure 3B,3C). The distribution of AITC-administered ovariectomized mice (OVX + AITC (1) and OVX + AITC (10) groups) was intermediate between that of the sham and OVX groups. PC (18:0/22:6) and PE (18:0/



https://doi.org/10.1021/acsomega.3c06622
ACS Omega 2023, 8, 43118−43129

Table 1. Principal Component Score of Phospholipids Containing DHA[a]

| hippocampus | PC1 (39.86%) | PC2 (15.1%) |
|---|---|---|
| PC(18:1/22:6) | 2.31 | −2.94 |
| PE(p-16:0/22:6) | 2.79 | 0.80 |
| PE(p-18:0/22:6) | 3.31 | 1.17 |
| PC(18:0/22:6) | 3.34 | −1.14 |
| PS(16:0/22:6) | 4.08 | 0.91 |
| PE(18:0/22:6) | 4.75 | −1.31 |
| PE(16:0/22:6) | 4.79 | 0.62 |
| PC(16:0/22:6) | 4.87 | −1.56 |
| PE(18:1/22:6) | 5.02 | −0.51 |
| cerebral cortex | PC2 (23.39%) | PC 4 (4.42%) |
| PC(18:0/22:6) | −5.08 | 0.35 |
| PC(18:1/22:6) | −4.67 | 1.61 |
| PC(16:0/22:6) | −4.57 | −0.90 |
| PE(18:0/22:6) | −3.94 | 1.03 |
| PE(16:0/22:6) | −3.51 | −0.02 |
| PE(p-16:0/22:6) | −2.59 | 1.64 |
| PE(18:1/22:6) | −2.49 | 0.52 |
| PE(p-18:1/22:6) | −0.39 | 2.17 |
| PS(16:0/22:6) | 0.82 | −1.86 |
| liver | PC2 (16.41%) | PC3 (10.76%) |
| PE(18:0/22:6) | −4.25 | 0.59 |
| PC(18:0/22:6) | −4.07 | −1.97 |
| PE(16:0/22:6) | −3.93 | 1.79 |
| PS(16:0/22:6) | −3.86 | −0.28 |
| PC(16:0/22:6) | −3.43 | 0.75 |
| PE(18:1/22:6) | 0.53 | 0.07 |
| PC(18:1/22:6) | 1.58 | −2.62 |

[a]Principle component scores of glycerophospholipids containing DHA detected in lipidomics analysis of hippocampus, cerebral cortex, and liver shown in Figure 3 were summarized.

22:6) were strong contributors to PC2 in the cerebral cortex and liver (Table 1). Additionally, the levels of PC (16:0/22:6) and PE (16:0/22:6) in the hippocampus and liver and PE (18:0/22:6) in the hippocampus, cerebral cortex, and liver were significantly reduced by OVX when compared to Sham or Sham + AITC (Figure 4). These results indicated that AITC induced DHA-acylated phospholipids, especially PC (16:0/22:6), PE (16:0/22:6), and PE (18:0/22:6) in the brain (hippocampus and cerebral cortex) and liver, which may contribute to the improvement of cognitive decline observed in OVX mice.

**Expression Levels of Genes Associated with DHA Metabolism.** To investigate the molecular mechanism of DHA-acylated phospholipid biosynthesis, the expression of genes involved in DHA was determined. The expression of genes involved in DHA and DHA-acylated phospholipid biosynthesis, including fatty acid elongase (*Elovl2* and *Elovl5*), fatty acid desaturase (*Fads1* and *Fads2*), 1-acylglycerol-3-phosphate O-acyltransferase 3/lysophospholipid acyltransferase (*Agpat3*/*Lpaat3*), and acyl-CoA synthetase long-chain family member 6 (*Acsl6*), was determined. Although no significant differences were observed in the genes we tested, the expression of *Elovl2* and *Elovl5* in the liver was slightly decreased by OVX, which appeared to be improved by 1 mg/kg AITC treatment (Figure 5). Although the hepatic expression of *Acsl6* was below the detection limit, *Acsl6* in the brain tended to be increased by AITC in sham and OVX mice. These results suggest that AITC-induced DHA-acylated phospholipids in the brain might be regulated by *Elovl2* and *Elovl5* in the liver and *Acsl6*-mediated acyl-CoA biosynthesis in the brain.

## DISCUSSION

Low-temperature-induced fatty acid desaturation is widely conserved among organisms.[33−35] We evaluated whether AITC, a strong agonist of TRPA1, influences the lipid composition *in vitro* and *in vivo*. *In vitro* analysis using TRPA1-expressing HEK cells revealed that AITC increased the number of PUFA-acylated phospholipids, including PC (16:0/22:6) and PE (16:0/22:6), depending on the TRPA1 pathway (Figure 1). Meanwhile, in the *in vivo* analysis, DHA-acylated phospholipids, including PC (18:0/22:6) and PE (18:0/22:6), were increased in the liver and brain of AITC-administered mice (Figure 3 and Table 1). As DHA plays an important role in brain development, maintenance, and functions, DHA-acylated phospholipid induction by AITC might contribute to the amelioration of cognitive function decline in OVX mice (Figure 2). These results indicate that not only DHA uptake from dietary supplements but also the enhancement of inherent abilities to up-regulate DHA-containing lipids may be a potential strategy for mild cognitive impairment in aging.

TRPA1 is a member of the large TRP family of ion channels and functions as a $Ca^{2+}$ permeable nonselective cation channel. TRPA1 is expressed in sensory neurons, including the dorsal root and trigeminal ganglion. Although the expression was very low, TRPA1 mRNA and protein are also expressed in many other organs and tissues, including the brain, liver, heart, small intestine, lung, skeletal muscle, and pancreas.[63] TRPA1 therefore plays several roles in many different cell processes, including the central nervous system, cardiovascular system, gastrointestinal tract, and respiratory system.[64] Interestingly, TRPA1 knockout mice showed significant memory loss in the novel object recognition test and radial arm maze test.[65] Additionally, it has been reported that orally administered 6-MSITC, one of the other ITCs, reached the brain.[46] Therefore, the molecular mechanisms of AITC-induced DHA-acylated phospholipids in mice are at least partly mediated by TRPA1 in the liver and brain rather than *via* the vagus nerve in the neuronal system.

DHA is an essential fatty acid in animals. Therefore, either dietary uptake or synthesis from precursor *n*-3 fatty acids, including ALA and EPA, is necessary. In the case of biosynthesis from *n*-3 fatty acids, precursor fatty acids are metabolized by sequential enzymatic processes, such as desaturation, elongation, and *β*-oxidation, to form DHA. Although these enzyme genes are expressed in several tissues,[66] DHA biosynthesis is mainly performed in the liver.[67] The transformation ratio of orally administered ALA to DHA was very low (less than 5%), which was not sufficient to maintain the required DHA level. Additionally, these enzymatic processes for DHA biosynthesis compete with the abundant n-6 PUFA, linoleic acid (18:2). Therefore, it is recommended to use DHA itself to obtain the concentration required for human health.[40] While it is clear that plasma unesterified DHA can enter the brain,[68,69] DHA-lysoPC appears to be a preferred source of DHA for the brain.[70] It has been reported that DHA-lysoPC accumulates in the brain 10 times more than free-DHA.[71,72] Brain DHA is concentrated in the gray matter, which has been observed to lose volume owing to cognitive impairment, depression, and aging.[41,73] The brain requires a constant supply of DHA from the blood to replace DHA


https://doi.org/10.1021/acsomega.3c06622
ACS Omega 2023, 8, 43118−43129

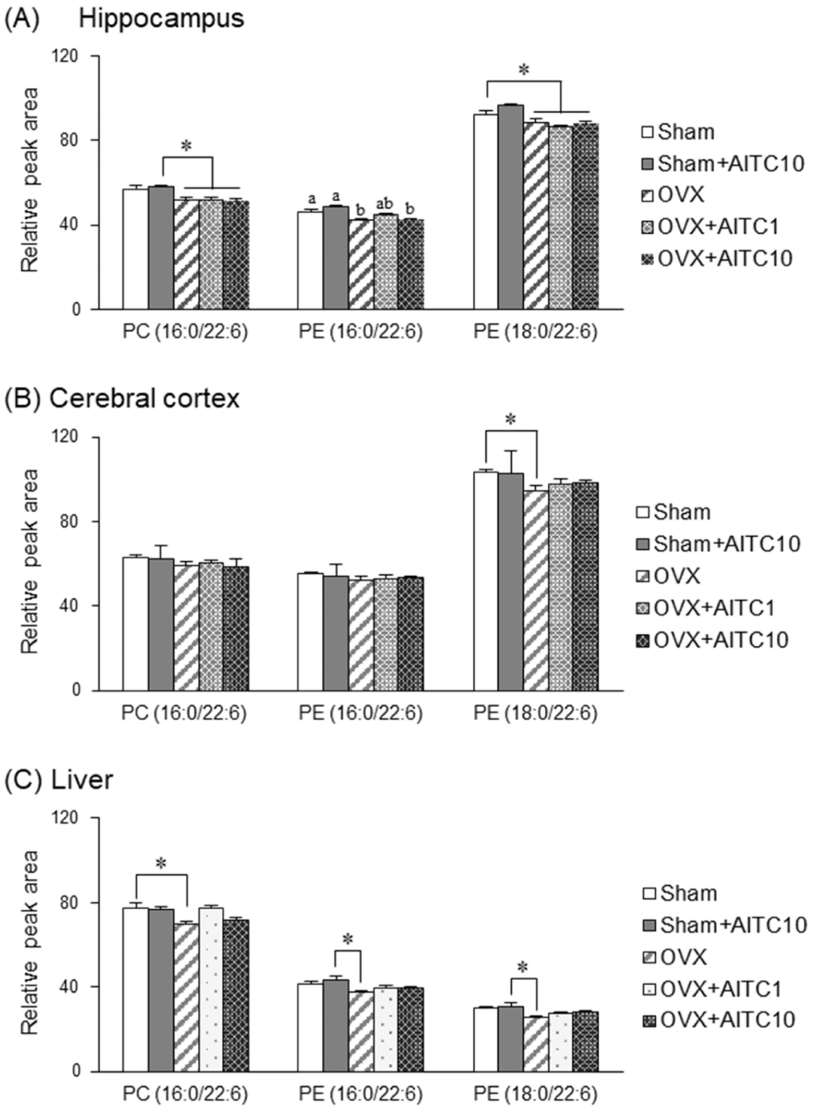


**Figure 4.** Levels of phosphatidylcholine (PC) and phosphatidylethanolamines (PE) containing acylated DHA. Relative levels of PC (16:0/22:6), PE (16:0/22:6), and PE (18:0/22:6) in the (A) hippocampus, (B) cerebral cortex, and (C) liver after the intragastric injections of AITC (0, 1, or 10 mg/kg body weight) for 18 d into the sham and OVX mice are shown. Values are represented as the mean ± SEM ($n$ = 6 or 7). Statistical significance was determined by one-way ANOVA followed by Tukey HSD post hoc test. *$P < 0.05$. Bars designated with the same letter are not statistically different ($P \geq 0.05$).

consumed in metabolic reactions. Fernandez et al. recently found that ACSL6, a member of the long-chain acyl-CoA synthetase (ACSL) family, is essential for enriching brain DHA, and ACSL6 knockout in mice affected motor function, memory, and age-related neuroinflammation in mice.[74,75] Here, we showed that the expression of ACSL6 in the hippocampus was slightly upregulated on AITC administration (Figure 5). There are no reports on the functional food factors that induce ACSL6. Therefore, our results may indicate that the ACSL6 could be a potential target to maintain the brain DHA. Moreover, DHA biosynthesis, hepatic excretion, transport, and uptake into the brain may be promising targets for exploring functional foods for brain functions. DHA-acylated PC and PE are critical biomarkers for screening for promising compounds in cell culture systems. The levels of DHA-containing phospholipids in the brain and liver were downregulated by OVX, and their levels were rescued by AITC administration (Figure 4). In contrast, total DHA levels in brain, liver, and plasma may have been affected by OVX and AITC administration but were not statistically different between experimental groups (Supporting Figure S3). These results suggest that AITC could activate the reconstitution of DHA-containing phospholipids in the brain, rather than DHA biosynthesis enzymes, including *Elovl*2/5 and *Fads1*/2. Further analyses are required to clarify which form of DHA is present in the brain (free-DHA, DHA-GP, and DHA-lysoGP, etc.) to discuss how increasing DHA-GP protects against cognitive decline without changing total DHA. Additionally, since TRPA1 increases cellular $Ca^{2+}$ levels, $Ca^{2+}$-dependent phospholipase $A_2$ activation may be associated with the reconstitution of DHA-phospholipid. Interestingly, Wu et al. reported that curcumin, a component of the spice turmeric, induced DHA synthesizing enzymes, FADS2 and elongase 2, resulting in the induction of DHA biosynthesis from its precursor, $\alpha$-linolenic acid (C18:3 $n$-3; ALA), in both liver and brain tissues.[76] The combination of ALA (2.7% in fat) and curcumin (500 ppm in the diet) increased 1.5-fold DHA in the rat liver and brain. In contrast, a single treatment with


https://doi.org/10.1021/acsomega.3c06622
ACS Omega 2023, 8, 43118−43129

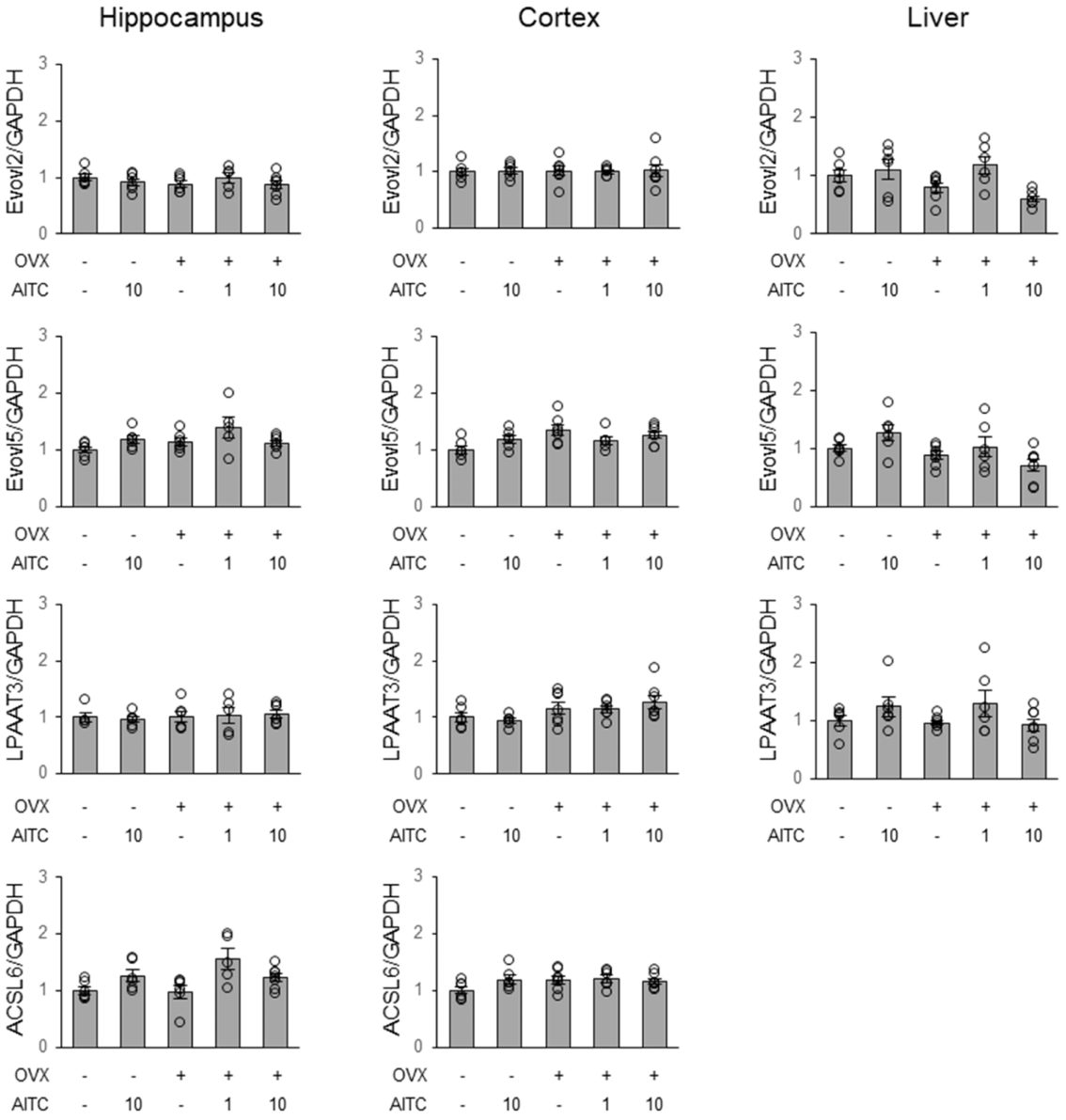


**Figure 5.** Gene expression levels in AITC-administered sham and OVX mice. After the intragastric injections of AITC (0, 1, or 10 mg/kg body weight) for 18 d, total RNA in the hippocampus, cortex, and liver were extracted from the sham and OVX mice. Relative gene expression were analyzed by reverse transcription-quantitative polymerase chain reaction. Mean value (open bars) with individual data (plots, $n$ = 5−7) are shown. Statistical significance was not observed by one-way ANOVA.

curcumin or ALA induced DHA in the liver but not in the brain. It was also argued that *in vivo* cotreatment with curcumin and ALA improved anxiety-like behavior in SD rats.[76] In the current study, all mice were fed the MF diet during the experimental period, so the influence of dietary ALA supply could not be evaluated. Therefore, the cotreatment of DHA precursors with stimulators, such as curcumin or AITC, may be more efficient in supplying DHA to the brain. The co-ingestion of DHA precursors and biosynthesizers may be an important strategy for maintaining brain function.

A recent animal study demonstrated that 6-MSITC improved impaired cognition in Alzheimer's disease model $App^{NLGF}$ mice by antioxidative and anti-inflammatory activities *via* the Nrf2-Keap1 pathway.[46] The levels of some plasmalogen phosphatidylethanolamine (PlsPE) molecules containing DHA, such as PlsPE (d16:0/22:6) and (d18:0/22:6), were significantly decreased in the brains of Alzheimer's disease model $APP^{NLGF}$ mice (hippocampi). However, the decline in these lipid molecules was rescued in the genetic Nrf2 induction model ($APP^{NLGF}$::$Keap1^{FA/FA}$ mice), although the physiological significance of PlsPE-containing DHA has not been fully elucidated.[46] Since Nrf2-induced antioxidative and anti-inflammatory properties may also result in the upregulation of DHA-containing lipids, further analysis is required to determine the involvement of the Keap1-Nrf2 pathway in AITC-induced cognitive repair. Additionally, in the current study, DHA-acylated phospholipids were downregulated in the brain and liver of OVX mice. Since estrogens are plausible regulators of DHA concentration in humans[77] and fish,[78] steroidal sex hormone homeostasis could be another target to regulate DHA biosynthesis and brain function. Since DHA biosynthesis in the liver has been reported to be higher in females,[79] it may be necessary to confirm whether AITC induces DHA-acylated phospholipids in the male brain.



https://doi.org/10.1021/acsomega.3c06622
*ACS Omega* 2023, 8, 43118−43129

Taken together, we showed that AITC induced DHA-containing phospholipids *in vitro* and *in vivo*. Moreover, the AITC-activating TRPA1 signaling pathway mediated the desaturation of fatty acids acylated with phospholipids. Several clinical trials are currently underway to assess the effects of ITCs on brain cognitive functions.[80,81] One study reported showed that 12 weeks of intervention with sulforaphane, a promising ITC, significantly improved cognitive function.[82] Therefore, AITC-induced DHA phospholipids may prevent cognitive function decline; however, the underlying molecular mechanism requires further investigation.

## ■ ASSOCIATED CONTENT

### Supporting Information

The Supporting Information is available free of charge at https://pubs.acs.org/doi/10.1021/acsomega.3c06622.

> Fatty acid composition in MF diet used in this study (Table S1); list of 52 phospholipids identified in HEK_hTRPA1 cells (Table S2); effects of AITC on the gene expression levels of NAD(P)H quinone oxidoreductase 1 (NQO1), glutamate-cysteine ligase catalytic subunit (GCLC), and glutathione S-transferase (GST)-P1 in HEK_hTRPA1 cells (Figure S1); body weight and weights of the hippocampus and cerebral cortex (Figure S2); and fatty acid composition in AITC-administered sham and OVX mice (Figure S3) (PDF)

## ■ AUTHOR INFORMATION


### Corresponding Author

**Noriyuki Miyoshi** − *Graduate School of Integrated Pharmaceutical and Nutritional Sciences, University of Shizuoka, Shizuoka 4228526, Japan*; orcid.org/0000-0002-4233-4282; Phone: +81-54-264-5531; Email: miyoshin@u-shizuoka-ken.ac.jp

### Authors

**Akika Nagata** − *Graduate School of Integrated Pharmaceutical and Nutritional Sciences, University of Shizuoka, Shizuoka 4228526, Japan*

**Shiori Oishi** − *Graduate School of Integrated Pharmaceutical and Nutritional Sciences, University of Shizuoka, Shizuoka 4228526, Japan*

**Nanako Kirishita** − *Graduate School of Integrated Pharmaceutical and Nutritional Sciences, University of Shizuoka, Shizuoka 4228526, Japan*

**Keita Onoda** − *Graduate School of Integrated Pharmaceutical and Nutritional Sciences, University of Shizuoka, Shizuoka 4228526, Japan*

**Takuma Kobayashi** − *Graduate School of Integrated Pharmaceutical and Nutritional Sciences, University of Shizuoka, Shizuoka 4228526, Japan*

**Yuko Terada** − *Graduate School of Integrated Pharmaceutical and Nutritional Sciences, University of Shizuoka, Shizuoka 4228526, Japan*

**Akira Minami** − *Department of Biochemistry, School of Pharmaceutical Sciences, University of Shizuoka, Shizuoka 4228526, Japan*

**Nanami Senoo** − *Graduate School of Integrated Pharmaceutical and Nutritional Sciences, University of Shizuoka, Shizuoka 4228526, Japan*

**Yasukiyo Yoshioka** − *Graduate School of Integrated Pharmaceutical and Nutritional Sciences, University of Shizuoka, Shizuoka 4228526, Japan*

**Kunitoshi Uchida** − *Graduate School of Integrated Pharmaceutical and Nutritional Sciences, University of Shizuoka, Shizuoka 4228526, Japan*

**Keisuke Ito** − *Graduate School of Integrated Pharmaceutical and Nutritional Sciences, University of Shizuoka, Shizuoka 4228526, Japan*

**Shinji Miura** − *Graduate School of Integrated Pharmaceutical and Nutritional Sciences, University of Shizuoka, Shizuoka 4228526, Japan*

Complete contact information is available at: https://pubs.acs.org/10.1021/acsomega.3c06622


### Author Contributions

N.M. designed the experiments. A.N. performed the *in vitro* assay using TRPA1-expressing HEK cells. A.N., S.O., N.K., K.O., and T.K. performed LC-MS and RT-qPCR. A.N., K.O., T.K., and A.M. performed the Morris water maze test. N.M. interpreted the data and wrote the manuscript with Y.T., A.M., N.S., Y.Y., K.U., K.I., and S.M. All authors have reviewed the manuscript.

### Notes

The authors declare no competing financial interest.

## ■ ACKNOWLEDGMENTS

The authors thank Dr. Tsutomu Hashidume for his technical support. This work was supported in part by a Grant-in-Aid for Scientific Research (KAKENHI, No. 20H04109 to NM) from the Japanese Ministry of Education, Culture, Sports, Science, and Technology (MEXT, Tokyo) and by the Food and Healthcare Open Innovation Project of Shizuoka Prefecture.

## ■ REFERENCES


(1) Nakamura, Y.; Miyoshi, N. Electrophiles in Foods: The Current Status of Isothiocyanates and Their Chemical Biology. *Biosci. Biotechnol. Biochem.* **2010**, *74* (2), 242−255, DOI: 10.1271/bbb.90731.

(2) Nakamura, Y.; Miyoshi, N. Cell Death Induction by Isothiocyanates and Their Underlying Molecular Mechanisms. *BioFactors* **2006**, *26* (2), 123−134, DOI: 10.1002/biof.5520260203.

(3) Vanduchova, A.; Anzenbacher, P.; Anzenbacherova, E. Isothiocyanate from Broccoli, Sulforaphane, and Its Properties. *J. Med. Food* **2019**, *22* (2), 121−126.

(4) Keum, Y.-S.; Jeong, W.-S.; Kong, A.-N. T. Chemopreventive Functions of Isothiocyanates. *Drug News Perspect.* **2005**, *18* (7), 445−451.

(5) Keum, Y.-S.; Jeong, W.-S.; Kong, A. N. T. Chemoprevention by Isothiocyanates and Their Underlying Molecular Signaling Mechanisms. *Mutat. Res., Fundam. Mol. Mech. Mutagen.* **2004**, *555* (1−2), 191−202.

(6) Gupta, P.; Wright, S. E.; Kim, S.-H.; Srivastava, S. K. Phenethyl Isothiocyanate: A Comprehensive Review of Anti-Cancer Mechanisms. *Biochim. Biophys. Acta* **2014**, *1846* (2), 405−424.

(7) Gwon, M.-H.; Im, Y.-S.; Seo, A.-R.; Kim, K. Y.; Moon, H.-R.; Yun, J.-M. Phenethyl Isothiocyanate Protects against High Fat/Cholesterol Diet-Induced Obesity and Atherosclerosis in C57BL/6 Mice. *Nutrients* **2020**, *12* (12), No. 3657, DOI: 10.3390/nu12123657.

(8) Chuang, W.-T.; Liu, Y.-T.; Huang, C.-S.; Lo, C.-W.; Yao, H.-T.; Chen, H.-W.; Lii, C.-K. Benzyl Isothiocyanate and Phenethyl Isothiocyanate Inhibit Adipogenesis and Hepatosteatosis in Mice with Obesity Induced by a High-Fat Diet. *J. Agric. Food Chem.* **2019**, *67* (25), 7136−7146.

(9) Yagi, M.; Nakatsuji, Y.; Maeda, A.; Ota, H.; Kamikubo, R.; Miyoshi, N.; Nakamura, Y.; Akagawa, M. Phenethyl Isothiocyanate Activates Leptin Signaling and Decreases Food Intake. *PLoS One* **2018**, *13* (11), No. e0206748.
(10) Choi, K.-M.; Lee, Y.-S.; Kim, W.; Kim, S. J.; Shin, K.-O.; Yu, J.-Y.; Lee, M. K.; Lee, Y.-M.; Hong, J. T.; Yun, Y.-P.; Yoo, H.-S. Sulforaphane Attenuates Obesity by Inhibiting Adipogenesis and Activating the AMPK Pathway in Obese Mice. *J. Nutr. Biochem.* **2014**, *25* (2), 201−207.
(11) Conzatti, A.; da Silva Fróes, T.; Carolina, F.; Perry, S.; et al. Clinical and Molecular Evidence of the Consumption of Broccoli, Glucoraphanin and Sulforaphane in Humans. *Nutr. Hosp.* **2014**, *31* (2), 559−569, DOI: 10.3305/nh.2015.31.2.7685.
(12) Axelsson, A. S.; Tubbs, E.; Mecham, B.; Chacko, S.; Nenonen, H. A.; Tang, Y.; Fahey, J. W.; Derry, J. M. J.; Wollheim, C. B.; Wierup, N.; Haymond, M. W.; Friend, S. H.; Mulder, H.; Rosengren, A. H. Sulforaphane Reduces Hepatic Glucose Production and Improves Glucose Control in Patients with Type 2 Diabetes. *Sci. Transl. Med.* **2017**, *9* (394), No. eaah4477, DOI: 10.1126/scitranslmed.aah4477.
(13) Yamagishi, S.-I.; Matsui, T. Protective Role of Sulphoraphane against Vascular Complications in Diabetes. *Pharm. Biol.* **2016**, *54* (10), 2329−2339.
(14) Nakamura, T.; Abe-Kanoh, N.; Nakamura, Y. Physiological Relevance of Covalent Protein Modification by Dietary Isothiocyanates. *J. Clin. Biochem. Nutr.* **2018**, *62* (1), 11−19.
(15) Baird, L.; Yamamoto, M. The Molecular Mechanisms Regulating the KEAP1-NRF2 Pathway. *Mol. Cell. Biol.* **2020**, *40* (13), No. e00099-20, DOI: 10.1128/MCB.00099-20.
(16) Mi, L.; Xiao, Z.; Hood, B. L.; Dakshanamurthy, S.; Wang, X.; Govind, S.; Conrads, T. P.; Veenstra, T. D.; Chung, F.-L. Covalent Binding to Tubulin by Isothiocyanates. A Mechanism of Cell Growth Arrest and Apoptosis. *J. Biol. Chem.* **2008**, *283* (32), 22136−22146.
(17) Xiao, Z.; Mi, L.; Chung, F.-L.; Veenstra, T. D. Proteomic Analysis of Covalent Modifications of Tubulins by Isothiocyanates. *J. Nutr.* **2012**, *142* (7), 1377S−1381S.
(18) Cross, J. V.; Rady, J. M.; Foss, F. W.; Lyons, C. E.; Macdonald, T. L.; Templeton, D. J. Nutrient Isothiocyanates Covalently Modify and Inhibit the Inflammatory Cytokine Macrophage Migration Inhibitory Factor (MIF). *Biochem. J.* **2009**, *423* (3), 315−321.
(19) Brown, K. K.; Blaikie, F. H.; Smith, R. A. J.; Tyndall, J. D. A.; Lue, H.; Bernhagen, J.; Winterbourn, C. C.; Hampton, M. B. Direct Modification of the Proinflammatory Cytokine Macrophage Migration Inhibitory Factor by Dietary Isothiocyanates. *J. Biol. Chem.* **2009**, *284* (47), 32425−32433.
(20) Miyoshi, N.; Yonemochi, T.; Tomono, S.; Fukutomi, R.; Nakamura, Y.; Ohshima, H. Development and Application of a Method for Identification of Isothiocyanate-Targeted Molecules in Colon Cancer Cells. *Anal. Biochem.* **2012**, *429* (2), 124−131.
(21) Cross, J. V.; Foss, F. W.; Rady, J. M.; Macdonald, T. L.; Templeton, D. J. The Isothiocyanate Class of Bioactive Nutrients Covalently Inhibit the MEKK1 Protein Kinase. *BMC Cancer* **2007**, *7*, No. 183, DOI: 10.1186/1471-2407-7-183.
(22) Lin, R.-K.; Zhou, N.; Lyu, Y. L.; Tsai, Y.-C.; Lu, C.-H.; Kerrigan, J.; Chen, Y.; Guan, Z.; Hsieh, T.-S.; Liu, L. F. Dietary Isothiocyanate-Induced Apoptosis via Thiol Modification of DNA Topoisomerase II$\alpha$. *J. Biol. Chem.* **2011**, *286* (38), 33591−33600.
(23) Shibata, T.; Kimura, Y.; Mukai, A.; Mori, H.; Ito, S.; Asaka, Y.; Oe, S.; Tanaka, H.; Takahashi, T.; Uchida, K. Transthiocarbamoylation of Proteins by Thiolated Isothiocyanates. *J. Biol. Chem.* **2011**, *286* (49), 42150−42161.
(24) Nakamura, T.; Kawai, Y.; Kitamoto, N.; Osawa, T.; Kato, Y. Covalent Modification of Lysine Residues by Allyl Isothiocyanate in Physiological Conditions: Plausible Transformation of Isothiocyanate from Thiol to Amine. *Chem. Res. Toxicol.* **2009**, *22* (3), 536−542.
(25) Nakamura, T.; Kitamoto, N.; Osawa, T.; Kato, Y. Immunochemical Detection of Food-Derived Isothiocyanate as a Lysine Conjugate. *Biosci. Biotechnol. Biochem.* **2010**, *74* (3), 536−540.
(26) Macpherson, L. J.; Dubin, A. E.; Evans, M. J.; Marr, F.; Schultz, P. G.; Cravatt, B. F.; Patapoutian, A. Noxious Compounds Activate TRPA1 Ion Channels through Covalent Modification of Cysteines. *Nature* **2007**, *445* (7127), 541−545.
(27) Story, G. M.; Peier, A. M.; Reeve, A. J.; Eid, S. R.; Mosbacher, J.; Hricik, T. R.; Earley, T. J.; Hergarden, A. C.; Andersson, D. A.; Hwang, S. W.; McIntyre, P.; Jegla, T.; Bevan, S.; Patapoutian, A. ANKTM1, a TRP-like Channel Expressed in Nociceptive Neurons, Is Activated by Cold Temperatures. *Cell* **2003**, *112* (6), 819−829.
(28) Chen, J.; Hackos, D. H. TRPA1 as a Drug Target−Promise and Challenges. *Naunyn-Schmiedeberg's Arch. Pharmacol.* **2015**, *388* (4), 451−463.
(29) Takaya, J.; Mio, K.; Shiraishi, T.; Kurokawa, T.; Otsuka, S.; Mori, Y.; Uesugi, M. A Potent and Site-Selective Agonist of TRPA1. *J. Am. Chem. Soc.* **2015**, *137* (50), 15859−15864.
(30) Hinman, A.; Chuang, H.-H.; Bautista, D. M.; Julius, D. TRP Channel Activation by Reversible Covalent Modification. *Proc. Natl. Acad. Sci. U.S.A.* **2006**, *103* (51), 19564−19568.
(31) Arenas, O. M.; Zaharieva, E. E.; Para, A.; Vásquez-Doorman, C.; Petersen, C. P.; Gallio, M. Activation of Planarian TRPA1 by Reactive Oxygen Species Reveals a Conserved Mechanism for Animal Nociception. *Nat. Neurosci.* **2017**, *20* (12), 1686−1693.
(32) Melo, N.; Capek, M.; Arenas, O. M.; Afify, A.; Yilmaz, A.; Potter, C. J.; Laminette, P. J.; Para, A.; Gallio, M.; Stensmyr, M. C. The Irritant Receptor TRPA1Mediates the Mosquito Repellent Effect of Catnip. *Curr. Biol.* **2021**, *31* (9), 1988−1994.e5.
(33) Kawamoto, J.; Kurihara, T.; Yamamoto, K.; Nagayasu, M.; Tani, Y.; Mihara, H.; Hosokawa, M.; Baba, T.; Sato, S. B.; Esaki, N. Eicosapentaenoic Acid Plays a Beneficial Role in Membrane Organization and Cell Division of a Cold-Adapted Bacterium, Shewanella Livingstonensis Ac10. *J. Bacteriol.* **2009**, *191* (2), 632−640.
(34) Nejadsadeghi, L.; Maali-Amiri, R.; Zeinali, H.; Ramezanpour, S.; Sadeghzade, B. Membrane Fatty Acid Compositions and Cold-Induced Responses in Tetraploid and Hexaploid Wheats. *Mol. Biol. Rep.* **2015**, *42* (2), 363−372.
(35) Pan, Q.; Li, M.; Shi, Y.-L.; Liu, H.; Speakman, J. R.; Wang, D.-H. Lipidomics Reveals Mitochondrial Membrane Remodeling Associated with Acute Thermoregulation in a Rodent with a Wide Thermoneutral Zone. *Lipids* **2014**, *49* (7), 715−730.
(36) Shahidi, F.; Ambigaipalan, P. Omega-3 Polyunsaturated Fatty Acids and Their Health Benefits. *Annu. Rev. Food Sci. Technol.* **2018**, *9*, 345−381.
(37) Cholewski, M.; Tomczykowa, M.; Tomczyk, M. A Comprehensive Review of Chemistry, Sources and Bioavailability of Omega-3 Fatty Acids. *Nutrients* **2018**, *10* (11), No. 1662, DOI: 10.3390/nu10111662.
(38) Lauritzen, L.; Brambilla, P.; Mazzocchi, A.; Harsløf, L. B. S.; Ciappolino, V.; Agostoni, C. DHA Effects in Brain Development and Function. *Nutrients* **2016**, *8* (1), No. 6, DOI: 10.3390/nu8010006.
(39) Mallick, R.; Basak, S.; Duttaroy, A. K. Docosahexaenoic Acid,22:6n-3: Its Roles in the Structure and Function of the Brain. *Int. J. Dev. Neurosci.* **2019**, *79*, 21−31.
(40) Weiser, M. J.; Butt, C. M.; Mohajeri, M. H. Docosahexaenoic Acid and Cognition throughout the Lifespan. *Nutrients* **2016**, *8* (2), No. 99, DOI: 10.3390/nu8020099.
(41) McNamara, R. K.; Liu, Y.; Jandacek, R.; Rider, T.; Tso, P. The Aging Human Orbitofrontal Cortex: Decreasing Polyunsaturated Fatty Acid Composition and Associated Increases in Lipogenic Gene Expression and Stearoyl-CoA Desaturase Activity. *Prostaglandins, Leukotrienes Essent. Fatty Acids* **2008**, *78* (4−5), 293−304.
(42) Barceló-Coblijn, G.; Murphy, E. J. Alpha-Linolenic Acid and Its Conversion to Longer Chain n-3 Fatty Acids: Benefits for Human Health and a Role in Maintaining Tissue n-3 Fatty Acid Levels. *Prog. Lipid Res.* **2009**, *48* (6), 355−374.
(43) McGrattan, A. M.; McEvoy, C. T.; McGuinness, B.; McKinley, M. C.; Woodside, J. V. Effect of Dietary Interventions in Mild Cognitive Impairment: A Systematic Review. *Br. J. Nutr.* **2018**, *120* (12), 1388−1405.
(44) Quinn, J. F.; Raman, R.; Thomas, R. G.; Yurko-Mauro, K.; Nelson, E. B.; Van Dyck, C.; Galvin, J. E.; Emond, J.; Jack, C. R.;

Weiner, M.; Shinto, L.; Aisen, P. S. Docosahexaenoic Acid Supplementation and Cognitive Decline in Alzheimer Disease: A Randomized Trial. *JAMA* **2010**, *304* (17), 1903−1911.
(45) Arellanes, I. C.; Choe, N.; Solomon, V.; He, X.; Kavin, B.; Martinez, A. E.; Kono, N.; Buennagel, D. P.; Hazra, N.; Kim, G.; D'Orazio, L. M.; McCleary, C.; Sagare, A.; Zlokovic, B. V.; Hodis, H. N.; Mack, W. J.; Chui, H. C.; Harrington, M. G.; Braskie, M. N.; Schneider, L. S.; Yassine, H. N. Brain Delivery of Supplemental Docosahexaenoic Acid (DHA): A Randomized Placebo-Controlled Clinical Trial. *EBioMedicine* **2020**, *59*, No. 102883.
(46) Uruno, A.; Matsumaru, D.; Ryoke, R.; Saito, R.; Kadoguchi, S.; Saigusa, D.; Saito, T.; Saido, T. C.; Kawashima, R.; Yamamoto, M. Nrf2 Suppresses Oxidative Stress and Inflammation in App Knock-In Alzheimer's Disease Model Mice. *Mol. Cell. Biol.* **2020**, *40* (6), No. e00467-19, DOI: 10.1128/MCB.00467-19.
(47) Okumura, Y.; Narukawa, M.; Iwasaki, Y.; Ishikawa, A.; Matsuda, H.; Yoshikawa, M.; Watanabe, T. Activation of TRPV1 and TRPA1 by Black Pepper Components. *Biosci. Biotechnol. Biochem.* **2010**, *74* (5), 1068−1072.
(48) Terada, Y.; Yamashita, R.; Ihara, N.; Yamazaki-Ito, T.; Takahashi, Y.; Masuda, H.; Sakuragawa, S.; Ito, S.; Ito, K.; Watanabe, T. Human TRPA1 Activation by Terpenes Derived from the Essential Oil of Daidai, Citrus Aurantium L. Var. Daidai Makino. *Biosci. Biotechnol. Biochem.* **2019**, *83* (9), 1721−1728.
(49) Nakamura, T.; Miyoshi, N.; Ishii, T.; Nishikawa, M.; Ikushiro, S.; Watanabe, T. Activation of Transient Receptor Potential Ankyrin 1 by Quercetin and Its Analogs. *Biosci. Biotechnol. Biochem.* **2016**, *80* (5), 949−954.
(50) Miyoshi, N.; Iwasaki, N.; Tomono, S.; Higashi, T.; Ohshima, H. Occurrence of Cytotoxic 9-Oxononanoyl Secosterol Aldehydes in Human Low-Density Lipoprotein. *Free Radic. Biol. Med.* **2013**, *60*, 73−79.
(51) Tomono, S.; Yasue, Y.; Miyoshi, N.; Ohshima, H. Cytotoxic Effects of Secosterols and Their Derivatives on Several Cultured Cells. *Biosci. Biotechnol. Biochem.* **2013**, *77* (3), 651−653.
(52) Senoo, N.; Miyoshi, N.; Goto-Inoue, N.; Minami, K.; Yoshimura, R.; Morita, A.; Sawada, N.; Matsuda, J.; Ogawa, Y.; Setou, M.; Kamei, Y.; Miura, S. PGC-1$\alpha$-Mediated Changes in Phospholipid Profiles of Exercise-Trained Skeletal Muscle. *J. Lipid Res.* **2015**, *56* (12), 2286−2296.
(53) Senoo, N.; Akahori, T.; Ichida, H.; Miyoshi, N.; Morita, A.; Shimizu, T.; Shindou, H.; Miura, S. Fasting Increases 18:2-Containing Phosphatidylcholines to Complement the Decrease in 22:6-Containing Phosphatidylcholines in Mouse Skeletal Muscle. *PLoS One* **2021**, *16* (7), No. e0255178.
(54) Sanada, S.; Suzuki, T.; Nagata, A.; Hashidume, T.; Yoshikawa, Y.; Miyoshi, N. Intestinal Microbial Metabolite Stercobilin Involvement in the Chronic Inflammation of Ob/Ob Mice. *Sci. Rep.* **2020**, *10* (1), No. 6479.
(55) Hashidume, T.; Sakano, T.; Mochizuki, A.; Ito, K.; Ito, S.; Kawarasaki, Y.; Miyoshi, N. Identification of Soybean Peptide Leginsulin Variants in Different Cultivars and Their Insulin-like Activities. *Sci. Rep.* **2018**, *8* (1), No. 16847.
(56) Minami, A.; Mikami, Y.; Kano, T.; Matsushita, H.; Fujita, Y.; Yoshimura, M.; Abe, Y.; Watanabe, H.; Hara, M.; Kurebayashi, Y.; Takahashi, T.; Kanazawa, H.; Wakatsuki, A.; Suzuki, T. Mitigation of Memory Impairment in Ovariectomized Rats Using Garlic Powder Treated with Subcritical Water. *Biol. Pharm. Bull.* **2020**, *43* (3), 546−549.
(57) Djiogue, S.; Djeuda, A. B. D.; Etet, P. F. S.; Wanda, G. J. M. K.; Tadah, R. N. D.; Njamen, D. Memory and Exploratory Behavior Impairment in Ovariectomized Wistar Rats. *Behav. Brain Funct.* **2018**, *14* (1), No. 14, DOI: 10.1186/s12993-018-0146-7.
(58) Wu, W. W.; Bryant, D. N.; Dorsa, D. M.; Adelman, J. P.; Maylie, J. Ovarian Hormone Loss Impairs Excitatory Synaptic Transmission at Hippocampal CA3-CA1 Synapses. *J. Neurosci.* **2013**, *33* (41), 16158−16169.
(59) Kim, T.-W.; Kim, C.-S.; Kim, J.-Y.; Kim, C.-J.; Seo, J.-H. Combined Exercise Ameliorates Ovariectomy-Induced Cognitive Impairment by Enhancing Cell Proliferation and Suppressing Apoptosis. *Menopause* **2016**, *23* (1), 18−26.
(60) Monthakantirat, O.; Sukano, W.; Umehara, K.; Noguchi, H.; Chulikhit, Y.; Matsumoto, K. Effect of Miroestrol on Ovariectomy-Induced Cognitive Impairment and Lipid Peroxidation in Mouse Brain. *Phytomedicine* **2014**, *21* (11), 1249−1255.
(61) Kitson, A. P.; Marks, K. A.; Shaw, B.; Mutch, D. M.; Stark, K. D. Treatment of Ovariectomized Rats with 17$\beta$-Estradiol Increases Hepatic Delta-6 Desaturase Enzyme Expression and Docosahexaenoic Acid Levels in Hepatic and Plasma Phospholipids. *Prostaglandins, Leukotrienes Essent. Fatty Acids* **2013**, *89* (2−3), 81−88.
(62) Horrocks, L. A.; Yeo, Y. K. Health Benefits of Docosahexaenoic Acid (DHA). *Pharmacol. Res.* **1999**, *40* (3), 211−225.
(63) Stokes, A.; Wakano, C.; Koblan-Huberson, M.; Adra, C. N.; Fleig, A.; Turner, H. TRPA1 Is a Substrate for De-Ubiquitination by the Tumor Suppressor CYLD. *Cell. Signalling* **2006**, *18* (10), 1584−1594.
(64) Nilius, B.; Appendino, G.; Owsianik, G. The Transient Receptor Potential Channel TRPA1: From Gene to Pathophysiology. *Pflugers Arch. Eur. J. Physiol.* **2012**, *464* (5), 425−458.
(65) Payrits, M.; Borbely, E.; Godo, S.; Ernszt, D.; Kemeny, A.; Kardos, J.; Szoke, E.; Pinter, E. Genetic Deletion of TRPA1 Receptor Attenuates Amyloid Beta- 1−42 (A$\beta$1−42)-Induced Neurotoxicity in the Mouse Basal Forebrain in Vivo. *Mech. Ageing Dev.* **2020**, *189*, No. 111268.
(66) Wang, Y.; Botolin, D.; Christian, B.; Busik, J.; Xu, J.; Jump, D. B. Tissue-Specific, Nutritional, and Developmental Regulation of Rat Fatty Acid Elongases. *J. Lipid Res.* **2005**, *46* (4), 706−715.
(67) Igarashi, M.; DeMar, J. C.; Ma, K.; Chang, L.; Bell, J. M.; Rapoport, S. I. Docosahexaenoic Acid Synthesis from Alpha-Linolenic Acid by Rat Brain Is Unaffected by Dietary n-3 PUFA Deprivation. *J. Lipid Res.* **2007**, *48* (5), 1150−1158.
(68) Chen, C. T.; Kitson, A. P.; Hopperton, K. E.; Domenichiello, A. F.; Trépanier, M.-O.; Lin, L. E.; Ermini, L.; Post, M.; Thies, F.; Bazinet, R. P. Plasma Non-Esterified Docosahexaenoic Acid Is the Major Pool Supplying the Brain. *Sci. Rep.* **2015**, *5*, No. 15791.
(69) Umhau, J. C.; Zhou, W.; Carson, R. E.; Rapoport, S. I.; Polozova, A.; Demar, J.; Hussein, N.; Bhattacharjee, A. K.; Ma, K.; Esposito, G.; Majchrzak, S.; Herscovitch, P.; Eckelman, W. C.; Kurdziel, K. A.; Salem, N. Imaging Incorporation of Circulating Docosahexaenoic Acid into the Human Brain Using Positron Emission Tomography. *J. Lipid Res.* **2009**, *50* (7), 1259−1268.
(70) Nguyen, L. N.; Ma, D.; Shui, G.; Wong, P.; Cazenave-Gassiot, A.; Zhang, X.; Wenk, M. R.; Goh, E. L. K.; Silver, D. L. Mfsd2a Is a Transporter for the Essential Omega-3 Fatty Acid Docosahexaenoic Acid. *Nature* **2014**, *509* (7501), 503−506.
(71) Croset, M.; Brossard, N.; Polette, A.; Lagarde, M. Characterization of Plasma Unsaturated Lysophosphatidylcholines in Human and Rat. *Biochem. J.* **2000**, *345* (Pt 1), 61−67.
(72) Liu, L.; Bartke, N.; Van Daele, H.; Lawrence, P.; Qin, X.; Park, H. G.; Kothapalli, K.; Windust, A.; Bindels, J.; Wang, Z.; Brenna, J. T. Higher Efficacy of Dietary DHA Provided as a Phospholipid than as a Triglyceride for Brain DHA Accretion in Neonatal Piglets. *J. Lipid Res.* **2014**, *55* (3), 531−539.
(73) Karas, G. B.; Scheltens, P.; Rombouts, S. A. R. B.; Visser, P. J.; van Schijndel, R. A.; Fox, N. C.; Barkhof, F. Global and Local Gray Matter Loss in Mild Cognitive Impairment and Alzheimer's Disease. *NeuroImage* **2004**, *23* (2), 708−716.
(74) Fernandez, R. F.; Kim, S. Q.; Zhao, Y.; Foguth, R. M.; Weera, M. M.; Counihan, J. L.; Nomura, D. K.; Chester, J. A.; Cannon, J. R.; Ellis, J. M. Acyl-CoA Synthetase 6 Enriches the Neuroprotective Omega-3 Fatty Acid DHA in the Brain. *Proc. Natl. Acad. Sci. U.S.A.* **2018**, *115* (49), 12525−12530.
(75) Fernandez, R. F.; Pereyra, A. S.; Diaz, V.; Wilson, E. S.; Litwa, K. A.; Martínez-Gardeazabal, J.; Jackson, S. N.; Brenna, J. T.; Hermann, B. P.; Eells, J. B.; Ellis, J. M. Acyl-CoA Synthetase 6 Is Required for Brain Docosahexaenoic Acid Retention and Neuroprotection during Aging. *JCI Insight* **2021**, *6* (11), No. e144351, DOI: 10.1172/jci.insight.144351.

(76) Wu, A.; Noble, E. E.; Tyagi, E.; Ying, Z.; Zhuang, Y.; Gomez-Pinilla, F. Curcumin Boosts DHA in the Brain: Implications for the Prevention of Anxiety Disorders. *Biochim. Biophys. Acta* **2015**, *1852* (5), 951−961.
(77) Giltay, E. J.; Gooren, L. J. G.; Toorians, A. W. F. T.; Katan, M. B.; Zock, P. L. Docosahexaenoic Acid Concentrations Are Higher in Women than in Men Because of Estrogenic Effects. *Am. J. Clin. Nutr.* **2004**, *80* (5), 1167−1174.
(78) Higuchi, M.; Mekuchi, M.; Hano, T.; Imaizumi, H. Trans-Omics Analyses Revealed Differences in Hormonal and Nutritional Status between Wild and Cultured Female Japanese Eel (Anguilla Japonica). *PLoS One* **2019**, *14* (5), No. e0209063.
(79) Lassek, W. D.; Gaulin, S. J. C. Sex Differences in the Relationship of Dietary Fatty Acids to Cognitive Measures in American Children. *Front. Evol. Neurosci.* **2011**, *3*, No. 5, DOI: 10.3389/fnevo.2011.00005.
(80) Marino, M.; Martini, D.; Venturi, S.; Tucci, M.; Porrini, M.; Riso, P.; Del Bo', C. An Overview of Registered Clinical Trials on Glucosinolates and Human Health: The Current Situation. *Front. Nutr.* **2021**, *8*, No. 730906.
(81) Liu, F.; Huang, J.; Hei, G.; Wu, R.; Liu, Z. Effects of Sulforaphane on Cognitive Function in Patients with Frontal Brain Damage: Study Protocol for a Randomised Controlled Trial. *BMJ Open* **2020**, *10* (10), No. e037543.
(82) Nouchi, R.; Hu, Q.; Saito, T.; Kawata, N. Y. D. S.; Nouchi, H.; Kawashima, R. Brain Training and Sulforaphane Intake Interventions Separately Improve Cognitive Performance in Healthy Older Adults, Whereas a Combination of These Interventions Does Not Have More Beneficial Effects: Evidence from a Randomized Controlled Trial. *Nutrients* **2021**, *13* (2), No. 352, DOI: 10.3390/nu13020352.



https://doi.org/10.1021/acsomega.3c06622
*ACS Omega* 2023, 8, 43118−43129